

Chalcones: A Valid Scaffold for Monoamine Oxidases Inhibitors

Franco Chimenti,[†] Rossella Fioravanti,^{*,†} Adriana Bolasco,[†] Paola Chimenti,[†] Daniela Secci,[†] Francesca Rossi,[†] Matilde Yáñez,[‡] Francisco Orallo,[‡] Francesco Ortuso,[§] and Stefano Alcaro[§]

Dipartimento di Chimica e Tecnologie del Farmaco, Università degli Studi di Roma "La Sapienza", P. le A. Moro 5, 00185 Roma, Italy, Departamento de Farmacología and Instituto de Farmacia Industrial, Facultad de Farmacia, Universidad de Santiago de Compostela, Campus Universitario Sur, E-15782 Santiago de Compostela (La Coruña), Spain, Dipartimento di Scienze Farmacobiologiche, Università di Catanzaro "Magna Graecia", "Complesso Nini Barbieri", 88021 Roccella di Borgia (CZ), Italy

Received December 17, 2008

A large series of substituted chalcones have been synthesized and tested in vitro for their ability to inhibit human monoamine oxidases A and B (hMAO-A and hMAO-B). While all the compounds showed hMAO-B selective activity in the micro- and nanomolar ranges, the best results were obtained in the presence of chlorine and hydroxyl or methoxyl substituents. To better understand the enzyme–inhibitor interaction and to explain the selectivity of the most active compounds toward hMAO-B, molecular modeling studies were carried out on new, high resolution, hMAO-B crystallographic structures. For the only compound that also showed activity against hMAO-A as well as low selectivity, the molecular modeling study was also performed on the hMAO-A crystallographic structure. The docking technique provided new insight on the inhibition mechanism and the rational drug design of more potent/selective hMAO inhibitors based on the chalcone scaffold.

Introduction

Monoamine oxidases (MAOs; EC 1.4.3.4¹) are widespread enzymes responsible for the regulation and metabolism of major monoamine neurotransmitters (5-hydroxytryptamine (5-HT), norepinephrine, dopamine), modulating their concentrations in the brain and peripheral tissues. Two isoforms of MAOs were fully characterized:¹ hMAO-A and hMAO-B, according to their substrate specificity, inhibitor sensitivity, and amino acid sequence. Binda et al.^{2,3} described the crystal structure of these two subtypes, highlighting the selective interaction between them and their ligands. The researcher's interest in the rational design of potent, specific inhibitors with therapeutic potential and no undesirable side-effects has actually been renewed.⁴ As mentioned above, hMAOs play an important role in the metabolism of several neurotransmitters, and their inhibitors could be useful in the treatment of psychiatric and neurological diseases. Human MAO-B inhibitors are used alone or in combination in the therapy of Alzheimer's and Parkinson's diseases, and in 2006 a new MAO B inhibitor, safinamide, is about to enter phase III trials,⁵ while human MAO-A inhibitors are used as antidepressants and anti-anxiety agents.⁶ Furthermore, interest in selective inhibitors of hMAO-B has increased in recent years⁷ due to the discovery of an age-related increase in hMAO-B expression after

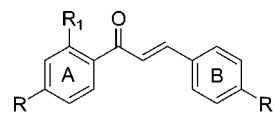


Figure 1. General chemical structure of synthesized *trans*-chalcones.

the 60th year of life especially in glial cells.^{8–10} Therefore, a selective hMAO-B inhibitor, could contribute to neuroprotection and prevent neuronal degeneration.¹¹

Because no general rules are available for the design of potent and selective inhibitors of hMAOs, in pursuing our studies in the field, we choose natural products as a significant source of new drug candidates. An impressive number of modern drugs have been developed from natural sources, especially from plants used as traditional folk medicine.

Chalcones (*trans*-1,3-diphenyl-2-propen-1-ones) are the biogenetic precursors of all known flavonoids and are abundant in edible plants.¹² Chemically, they consist of open-chain flavonoids in which the two aromatic rings are joined by a three-carbon α,β -unsaturated carbonyl system (Figure 1). They present a broad spectrum of biological activities^{12,13} such as anticancer, anti-inflammatory, antimalarial, antifungal,^{14,15} antilipidemic, and antiviral activities.¹⁶

For example, xanthoangelol has been reported to induce apoptosis and to inhibit tumor promotion and metastasis in several cancer cell lines.^{17,18} Brousochalcone A,¹⁹ dimethylaminochalcones,²⁰ and cardamonin²¹ possess anti-inflammatory activity.²² Licochalcone A, a substance found in the roots of the Chinese liquorice, showed antimalarial activity.²³ 4',4-Dichlorochalcone exhibits antilipidemic activity²⁴ (Figure 2).

There are other chalcones with very interesting biological activity such as butein²⁵ and isoliquiritigenin.²¹ These chalcones, like *trans*-resveratrol,²⁶ remarkably activate sirtuin²⁷ enzymatic activity, mimic the beneficial effects of caloric restriction (CR), retard the aging process, and increase longevity in the budding yeast *Saccharomyces cerevisiae*. However, the information on the inhibitory monoamine oxidase (MAO) activity of these

* To whom correspondence should be addressed. Phone. +39 06 49913975. Fax: +39 06 49913772. E-mail: rossella.fioravanti@uniroma1.it.

[†] Dipartimento di Chimica e Tecnologie del Farmaco, Università degli Studi di Roma "La Sapienza".

[‡] Departamento de Farmacología and Instituto de Farmacia Industrial, Facultad de Farmacia, Universidad de Santiago de Compostela.

[§] Dipartimento di Scienze Farmacobiologiche, Università di Catanzaro "Magna Graecia".

^a Abbreviations: MAO, monoamine oxidase; 5-HT (5-hydroxytryptamine); CR, caloric restriction; IC₅₀, 50% inhibitory concentration; Michaelis constant (K_m); maximum reaction velocity (V_{max}); MC, Monte Carlo; PDB, protein data bank; 2BXR and 2Z5X, PDB code of hMAO-A; 1GOS and 2BK3, PDB code of hMAO-B; FAD, flavin adenine dinucleotide; CVDW, Coulomb van der Waals; SEM, standard error of the mean; P, probability value; pIC₅₀ = -log IC₅₀. Abbreviations used for amino acids follow the rules of the IUPACIUB Commission of Biochemical Nomenclature in J. Biol. Chem. 1972, 247, 977–983. Amino acid symbols denote L-configuration unless indicated.

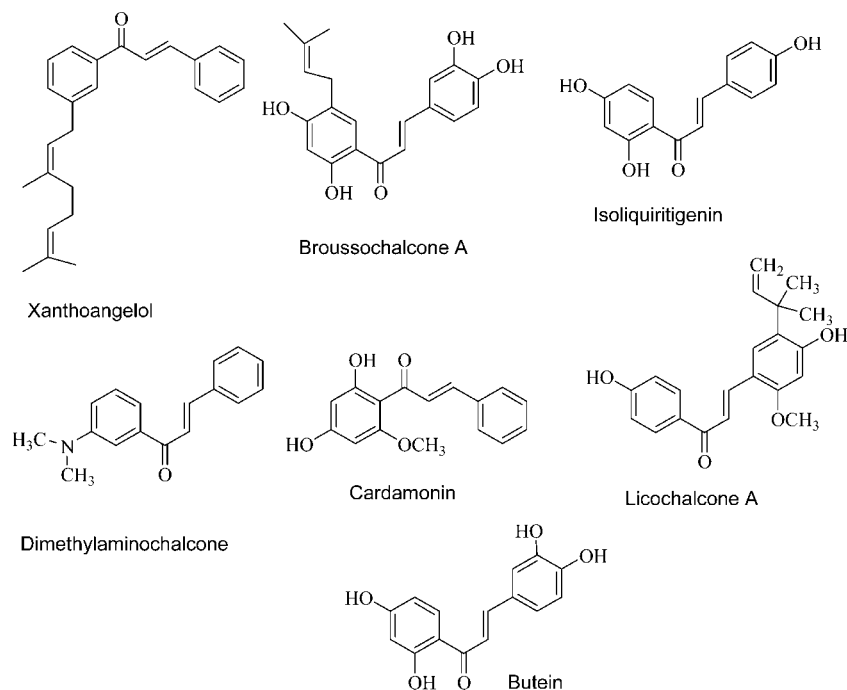


Figure 2. Structures of known *trans*-chalcones with biological activities.

molecules reported in the literature is limited and directed to behavioral tests and assays on rat mitochondrial MAOs.²⁸ Therefore, considering that chalcones are a structurally simple group of compounds that for our knowledge have not been assayed on human MAOs and that we previously^{29,30} reported a number of synthetic inhibitors of MAO-A and -B, in which chalcones are intermediate compounds, in this investigation we present the synthesis and the inhibitory activity against the A- and B-isoforms of hMAO of a number of substituted chalcones.

We also report on a computational study using the crystal structure data and models of hMAO-A and hMAO-B, deposited in the Protein Data Bank, with the aim of rationalizing the binding modes of these compounds with human MAO isoforms.

Chemistry

The general synthetic strategy employed to prepare chalcones in excellent yield (Table 1) was based on the Claisen–Schmidt condensation reported previously.³¹ By condensing substituted acetophenone with aromatic aldehydes, using solid barium hydroxide octahydrate as catalyst in methanol at 40 °C, we obtained derivatives **5** (Scheme 1). The starting materials were commercially available. This method for the preparation of chalcones is particularly attractive because it specifically generates the (*E*)-isomer.

Biochemistry

The potential effects of the test drugs on hMAO activity were investigated by measuring their effects on the production of hydrogen peroxide (H₂O₂) from *p*-tyramine using the Amplex Red MAO assay kit (Molecular Probes, Inc., Eugene, OR) and microsomal MAO isoforms prepared from insect cells (BTI-TN-5B1–4) infected with recombinant baculovirus containing cDNA inserts for hMAO-A or hMAO-B (Sigma-Aldrich Química SA, Alcobendas, Spain).

The production of H₂O₂ catalyzed by MAO isoforms can be detected using 10-acetyl-3,7-dihydroxyphenoxazine (Amplex Red reagent), a nonfluorescent and highly sensitive probe that reacts with H₂O₂ in the presence of horseradish peroxidase to

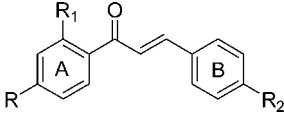
produce a fluorescent product, resorufin. In this study, hMAO activity was evaluated using the above method following the general procedure described previously by us.³² The test drugs (new compounds and reference inhibitors) themselves were unable to react directly with the Amplex Red reagent, which indicates that these drugs do not interfere with the measurements. In our experiments and under our experimental conditions, hMAO-A displayed a Michaelis constant (*K_m*) of 457.17 ± 38.62 μM and a maximum reaction velocity (*V_{max}*) of 185.67 ± 12.06 nmol/min/mg protein, whereas hMAO-B showed a *K_m* of 220.33 ± 32.80 μM and a *V_{max}* of 24.32 ± 1.97 nmol/min/mg protein (*n* = 5).

Most tested drugs inhibited this enzymatic control activity in a concentration-dependent way (see Table 1).

Results and Discussion

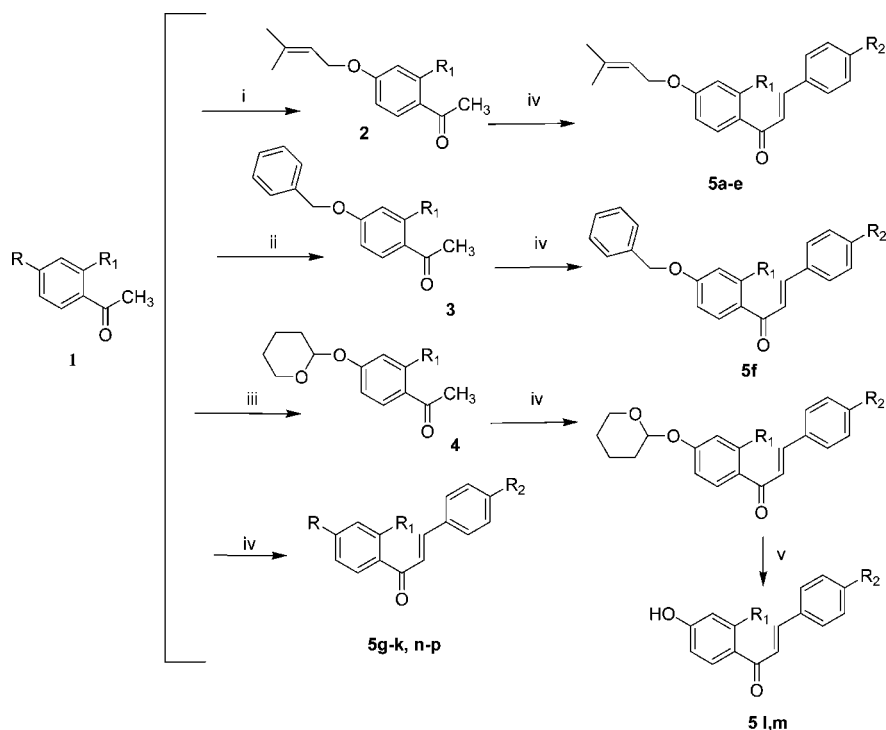
The hMAO-A and hMAO-B inhibition data are reported in Table 1 together with the selectivity index (selectivity index SI = IC₅₀ hMAO-A / IC₅₀ hMAO-B). It can be observed that all compounds show a selective inhibitory activity toward hMAO-B in the micro- and nanomolar range. The most active compounds, **5i** and **5m** (IC₅₀ = 0.0044 ± 0.00027 μM and 0.0051 ± 0.00019 μM, respectively), are disubstituted in the 2'- and 4'-position of the B aromatic moiety with two hydroxyls or hydroxyl and methoxy groups and in 4-position of the A aromatic moiety with a chlorine atom. Compound **5i** also shows the highest MAO-B selectivity (SI > 11364). The other compounds show good activity in the nanomolar range and selectivity, but among them the highest activity was detected for the compounds that are substituted with a chloro atom in the 4-position and with hydroxy or methoxy groups in the 4'-position. From this data, we can indicate that the presence in 2'- and 4'- position of the B aromatic moiety of the two previously indicated substituents and of a chlorine atom in 4-position of the A aromatic moiety is a fundamental requisite for inhibitory activity. The chalcones **5a–e**, 4'-isoprenyloxy substituted, show lower activity.

In the reversibility and irreversibility tests, h-MAO-B inhibition was irreversible in presence of the compounds **5a**, **5i**, and

Table 1. Structures and Inhibitory Activity of Derivatives **5a–p**


compd	R	R ₁	R ₂	hMAO-A (IC ₅₀ μM)	hMAO-B (IC ₅₀ μM) ^a	SI
5a	(CH ₃) ₂ C=CHCH ₂ O-	OH	H	**	18.76 ± 0.92	> 1.1 ^b
5b	(CH ₃) ₂ C=CHCH ₂ O-	OH	CH ₃	**	1.03 ± 0.09	> 19 ^b
5c	(CH ₃) ₂ C=CHCH ₂ O-	OH	OCH ₃	**	**	
5d	(CH ₃) ₂ C=CHCH ₂ O-	OH	OCH ₂ Ph	**	**	
5e	(CH ₃) ₂ C=CHCH ₂ O-	OH	Cl	**	1.25 ± 0.04	> 16 ^b
5f	OCH ₂ Ph	H	Cl	**	**	
5g	OCH ₃	H	Cl	**	0.054 ± 0.0033	> 370 ^b
5h	OCH ₃	H	OCH ₂ Ph	**	0.45 ± 0.028	> 44 ^b
5i	OCH ₃	OH	Cl	***	0.0044 ± 0.00027	> 11364 ^b
5j	H	H	H	**	1.41 ± 0.070	> 14 ^b
5k	H	OH	Cl	***	0.16 ± 0.0092	> 312 ^b
5l	OH	H	Cl	***	0.031 ± 0.00083	> 1613 ^b
5m	OH	OH	Cl	4.95 ± 0.28 ^a	0.0051 ± 0.00019	971
5n	F	OH	Cl	***	0.071 ± 0.0022	> 704 ^b
5o	F	H	OCH ₂ Ph	** ^c	0.50 ± 0.030	> 40 ^b
5p	SO ₂ CH ₃	H	Cl	** ^c	0.47 ± 0.017	> 43 ^b
A				0.0045 ± 0.00032 ^a	61.35 ± 1.13	0.000073
B				67.25 ± 1.02 ^a	0.020 ± 0.00086	3362
C				6.56 ± 0.76	7.54 ± 0.36	0.87
D				361.38 ± 19.37	*	< 0.36 ^c

SI: hMAO-B selectivity index = IC₅₀ (hMAO-A) / IC₅₀ (hMAO-B). Each IC₅₀ value is the mean ± S.E.M. from five experiments. * Inactive at 1mM (highest concentration tested). ** Inactive at 20 μM (highest concentration tested). *** Inactive at 50 μM (highest concentration tested). **A** = clorgyline; **B** = *R*-(−)-deprenyl; **C** = iproniazid; **D** = moclobemide. Level of statistical significance: ^a *P* < 0.01 versus the corresponding IC₅₀ values obtained against hMAO-B, as determined by ANOVA/Dunnett's. ^b Values obtained under the assumption that the corresponding IC₅₀ against MAO-A is the highest concentration tested (20 μM or 50 μM). ^c Value obtained under the assumption that the corresponding IC₅₀ against MAO-B is the highest concentration tested (1 mM).

Scheme 1^a

^a Reagents: (i) 3,3-dimethylallyl bromide, anhydrous K₂CO₃, acetone, rt; (ii) benzyl chloride, KI, Na₂CO₃, dry ethanol, refluxed; (iii) 3,4-dihydro-α-pyran, pyridinium *p*-toluenesulfonate, methylene chloride, rt; (iv) benzaldehyde, barium hydroxide octahydrate, methanol, 40° C; (v) *p*-toluenesulfonic acid, methanol, rt.

5m (chosen for docking experiments; see below) as shown by the lack of enzyme activity restoration after repeated washing. Similar results were obtained for *R*-(−)-deprenyl (Table 2).

With the aim of analyzing representatively the **5a**, **5i**, and **5m** binding modes, the most stable configurations of all complexes were graphically inspected (Figure 3).

Table 2. Reversibility and Irreversibility of hMAO-B Inhibition of Derivatives **5a**, **5m**, and **5i**^a

compd	% hMAO-B inhibition	
	before washing	after repeated washing
5a (20 μ M)	54.32 \pm 2.21	58.51 \pm 2.98
5m (5 nM)	55.12 \pm 3.67	61.38 \pm 4.26
5i (5 nM)	59.13 \pm 3.17	60.26 \pm 3.23
<i>R</i> -(-)-deprenyl (20 nM)	50.78 \pm 2.15	51.75 \pm 2.32

^a Each value is the mean \pm SEM from five experiments ($n = 5$).

Chalcone derivatives **5a**, **5i**, and **5m**, were selected on the basis of their experimentally demonstrated activity. In particular, **5a** was chosen because it was the least active compound, **5i** because it proved to be the most potent and selective, and **5m** because it was the only compound that showed affinity for both enzyme isoforms. Consequently, the molecular recognition of **5a** and **5i** was evaluated only with respect to hMAO-B isoform, while **5m** was analyzed against both isoenzymes.

The new Protein Data Bank (PDB)³³ high resolution crystallographic structures were considered as receptor models: 2Z5X³⁴ and 2BK3³⁵ for hMAO-A and hMAO-B, respectively.

The computational approach consisted of a preliminary conformational search of the ligands, followed by the flexible docking of global minimum energy conformers to the targets.

In agreement with the experimental data, all ligands showed productive recognition of the target. The hydroxy-phenyl ring was always placed toward the FAD cofactor. Its positioning, in the hMAOs active site, was strictly related to the substituents. The **5a** prenyloxy moiety hindrance prevented a deeper recognition of the hMAO-B binding cleft, while the smaller methoxy and hydroxyl groups, shown by **5i** and **5m**, allowed a fruitful interaction with the catalysis involved FAD and tyrosine amino acidic residues. In all cases, hydrogen bonds stabilized the recognition of the ligands. Such an observation was remarkable for the **5m**·hMAO-B complex, where two hydrogen bonds, with FAD and Tyr435, respectively, contributed to explain the greater activity of this inhibitor. The number of interacting residues was quite similar in all complexes (Table 3) and, on analyzing the different activities and selectivities, we attributed a pivotal role to Tyr326 in the hMAOs binding modes.

Because of its prenyloxy group, the less potent inhibitor **5a** was placed far from Tyr326 in hMAO-B simulations. The **5i** compound recognized Tyr326 well, while the most active inhibitor, **5m**, showed an H- π interaction through its chlorophenyl ring and two hydrogen bonds with other relevant residues (Figure 3). In hMAO-A, **5m** compound lost the contribution of Tyr326, which is altered in Ile335, and also that of other important amino acidic residues (Table 3). The resulting effect implied an experimental inhibition and a theoretical affinity that was quite similar to **5a** in hMAO-B. This scenario could be considered an explanation of the different behavior shown by **5a**, **5i**, and **5m** with respect to hMAOs inhibition.

Conclusion

In the present work, we have focused our attention onto the inhibitory activity of chalcones on hMAOs and demonstrate that they are more active and selective against the B-isoform; for these reasons, we can indicate chalcones as a useful scaffolds for hMAOs inhibitors and we plan to extend and report structure-activity relationship studies, including other substituents, in a further communication.

Experimental Section

Chemistry. Melting points are uncorrected and were determined on a Reichert Kofler thermopan apparatus. ¹H NMR spectra were

recorded on a Bruker AMX (300 MHz) using tetramethylsilane (TMS) as internal standard (chemical shifts in δ values, J in Hz). Elemental analyses for C, H, and N were determined with a Perkin-Elmer 240 B microanalyzer, and the analytical results were $\geq 95\%$ purity for all compounds.

Synthesis of 4'-Isoprenyloxy Acetophenone 2. 3,3-Dimethylallyl bromide (0.04 mol) was added dropwise to a mixture of 2,4-hydroxy acetophenone (0.03 mol) and anhydrous K₂CO₃ (0.04 mol) in acetone (100 mL). The mixture was stirred for 3 h at room temperature and then filtered. Removal of acetone from the filtrate left a residue, which was crystallized from petroleum ether to give a solid compound; mp 46–47 °C.

Synthesis of 4'-Benzyloxy Acetophenone 3. 4-Hydroxy acetophenone (0.022 mol), potassium iodide (300 mg), and sodium carbonate (0.022 mol) were stirred in dry ethanol (80 mL), after which benzyl chloride (0.022 mol) in dry ethanol (20 mL) was added dropwise. The reaction mixture was stirred and refluxed for 4 h. The reaction mixture was poured onto ice and the solid obtained was filtered, washed with water, and dried. The yielded crude residue 4'-benzyloxy acetophenone **3**, which was crystallized from ethanol; mp 82–83 °C.

Synthesis of 4'-Pyranosyl-2'-hydroxy Acetophenone 4. 2,4-Dihydroxyacetophenone (0.025 mol) and pyridinium *p*-toluenesulfonate (0.0006 mol) were stirred and reacted for 0.5 h in dichloromethane (80 mL), after which 3,4-dihydro- α -pyran (0.14 mol), dissolved in 20 mL of dichloromethane, was added dropwise. The reaction mixture was stirred at room temperature for 4 h and then was washed twice with water, dried, and evaporated in vacuo. The yielded crude residue, 4'-pyranosyl-2'-hydroxy acetophenone, was crystallized from petroleum ether to give a solid compound; mp 46–47 °C.

Synthesis of 4'-Isoprenyloxy Chalcones 5a–e. A solution of isoprenyloxy acetophenone **2** (0.01 mol) and the suitable benzaldehyde (0.01 mol) dissolved in ethanol was treated with barium hydroxide (0.01 mol). The solution was stirred for 24 h at 30 °C. After removal of ethanol, water was added to the residue and the solution was adjusted to pH 2 with diluted HCl and then extracted with chloroform. The organic layer was washed with water and then dried over anhydrous sodium sulfate. The removal of the chloroform left a solid, which was purified by crystallization from ethanol.

Synthesis of 4'-Benzyloxy Chalcones 5f. A solution of 4'-benzyloxy acetophenone **3** (0.01 mol) and the suitable benzaldehyde (0.01 mol) dissolved in ethanol was treated with barium hydroxide (0.01 mol). The solution was stirred for 24 h at 30 °C. After removal of ethanol, water was added to the residue and the solution was adjusted to pH 2 with diluted HCl and then extracted with chloroform. The organic layer was washed with water and then dried over anhydrous sodium sulfate. The removal of the chloroform left a solid, which was purified by crystallization from ethanol.

Synthesis of Chalcones 5g–k and 5n–p. A solution of acetophenone (0.025 mol), benzaldehyde (0.025 mol), and barium hydroxide octahydrate (0.025 mol) was dissolved in MeOH (100 mL). The reaction mixture was stirred for 12 h at 40 °C and then evaporated in vacuo. Water (100 mL) was added and the mixture was neutralized with HCl 2 M and extracted with EtOAc. The organic layer was separated, washed with water, and dried. The removal of the chloroform left a solid, which was purified by crystallization from a suitable solvent.

Synthesis of 2',4'-Dihydroxy Chalcones 5l–m. A solution of 4'-pyranosyl-2'-hydroxy acetophenone (0.01 mol) and the suitable benzaldehyde (0.01 mol) dissolved in ethanol was treated with barium hydroxide (0.01 mol). The solution was stirred for 24 h at 30 °C. After removal of ethanol, water was added to the residue and the solution was adjusted to pH 2 with diluted HCl and then extracted with chloroform. The organic layer was washed with water and then dried over anhydrous sodium sulfate. The crude product (0.025 mol) obtained after removal of the chloroform was dissolved in methanol with *p*-toluenesulfonic acid (0.025 mol). The reaction mixture was stirred for 4 h at room temperature and then evaporated in vacuo. The mixture was diluted with water (100 mL), neutralized

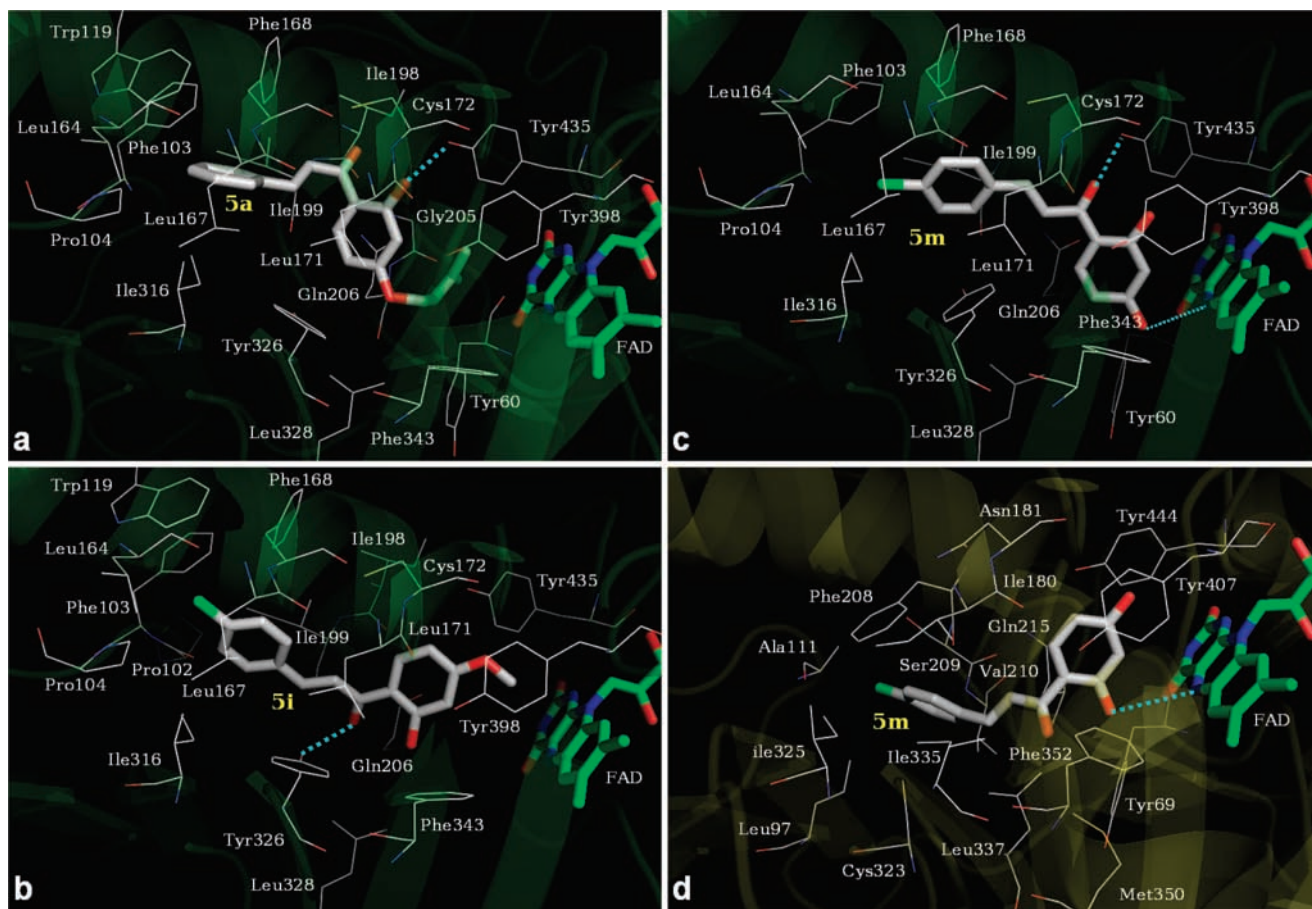


Figure 3. Most stable configuration of **5a**, **5i**, and **5m** into the hMAO-B (a–c) and **5m** into the hMAO-A (d) active sites. Hydrogen atoms are hidden for clarity, interacting residues are displayed in wireframe, ligand in sticks, FAD in sticks green carbon colored, and the rest of the enzymes are depicted in transparent green (hMAO-B) or yellow (hMAO-A) cartoon.

Table 3. Relevant Interacting Residues List for **5a**, **5i**, and **5m** hMAOs Recognition^a

corresponding residues		ligands			corresponding residues		ligands		
hMAO-A	hMAO-B	5a	5i	5m	hMAO-A	hMAO-B	5a	5i	5m
Tyr69	Tyr60	<i>b</i>	<i>ab</i>		Leu97	Leu88			<i>a</i>
Ala111	Pro102	<i>b</i>	<i>a</i>		Phe112	Phe103	<i>b</i>	<i>b</i>	<i>b</i>
Pro113	Pro104	<i>b</i>	<i>b</i>		Trp128	Trp119	<i>b</i>	<i>b</i>	
Phe173	Leu164	<i>b</i>	<i>b</i>		Leu176	Leu167	<i>b</i>	<i>b</i>	<i>b</i>
Phe177	Phe168	<i>b</i>	<i>b</i>		Ile180	Leu171	<i>b</i>	<i>b</i>	<i>ab</i>
Asn181	Cys172	<i>b</i>	<i>b</i>	<i>ab</i>	Ile207	Ile198	<i>b</i>	<i>b</i>	
Phe208	Ile199	<i>b</i>	<i>b</i>	<i>ab</i>	Ser209	Ser200			<i>a</i>
Val210	Thr201		<i>a</i>		Gly214	Gly205	<i>b</i>		
Gln215	Gln206	<i>b</i>	<i>b</i>	<i>ab</i>	Cys323	Thr314			<i>a</i>
Ile325	Ile316	<i>b</i>	<i>b</i>	<i>ab</i>	Ile335	Tyr326	<i>b</i>	<i>b+</i>	<i>ab</i>
Leu337	Leu328	<i>b</i>	<i>b</i>		Met350	Met341			<i>a</i>
Phe352	Phe343	<i>b</i>	<i>b</i>	<i>ab</i>	Tyr407	Tyr398	<i>b</i>	<i>b</i>	<i>ab</i>
Tyr444	Tyr435	<i>b+</i>	<i>b</i>	<i>ab+</i>	FAD	FAD	<i>b</i>	<i>b</i>	<i>a+b+</i>

^a *a*: hMAO-A interaction; *b*: hMAO-B interaction; +: hydrogen bond.

with 5% NaHCO₃ (50 mL), and extracted with EtOAc. The organic layer was separated, washed with water, dried, and evaporated in vacuo. The crude chalcones obtained were purified by crystallization from ethanol.

Determination of hMAO Isoform Activity. The effects of the test compounds on hMAO isoform enzymatic activity were evaluated at a fluorimetric method following the experimental protocol previously described by us.³²

Briefly, 0.1 mL of sodium phosphate buffer (0.05 M, pH 7.4) containing the test drugs (new compounds or reference inhibitors) in various concentrations and adequate amounts of recombinant hMAO-A or hMAO-B required and adjusted to obtain the same

reaction velocity in our experimental conditions, i.e., to oxidize (in the control group) the same concentration of substrate, were used: 165 pmol of *p*-tyramine/min (hMAO-A, 1.1 μg protein; specific activity, 150 nmol of *p*-tyramine oxidized to *p*-hydroxyphenylacetaldehyde/min/mg protein; hMAO-B, 7.5 μg protein; specific activity, 22 nmol of *p*-tyramine transformed/min/mg protein) were incubated for 15 min at 37 °C in a flat black-bottom 96-well microtest plate (BD Biosciences, Franklin Lakes, NJ) placed in a dark fluorimeter chamber. After this incubation period, the reaction was started by adding (final concentrations) 200 μM Amplex Red reagent, 1 U/mL horseradish peroxidase, and 1 mM *p*-tyramine. The production of H₂O₂ and, consequently, of resorufin, was quantified at 37 °C in a multidetection microplate fluorescence reader (FLX800, Bio-Tek Instruments, Inc., Winooski, VT) based on the fluorescence generated (excitation, 545 nm; emission, 590 nm) over a 15 min period, in which the fluorescence increased linearly.

Control experiments were carried out simultaneously by replacing the test drugs (new compounds and reference inhibitors) with appropriate dilutions of the vehicles. In addition, the potential ability of the test drugs to modify the fluorescence generated in the reaction mixture due to nonenzymatic inhibition (e.g., for directly reacting with Amplex Red reagent) was determined by adding these drugs to solutions containing only the Amplex Red reagent in a sodium phosphate buffer.

To determine the kinetic parameters of hMAO-A and hMAO-B (*K_m* and *V_{max}*), the corresponding enzymatic activity of both isoforms was evaluated (under the experimental conditions described above) in the presence of a number (a wide range) of *p*-tyramine concentrations.

The specific fluorescence emission (used to obtain the final results) was calculated after subtraction of the background activity,

Table 4. Comparison between Experimental pIC₅₀ and Theoretical Interaction Energy Values for Compounds **5a**, **5i**, and **5m**^a

compd	pIC ₅₀		Glide ECvdW	
	hMAO-A	hMAO-B	hMAO-A	hMAO-B
5a		4.73		-38.48
5i		8.35		-44.66
5m	5.31	8.30	-39.52	-43.25

^a ECvdW is reported in kcal/mol.

which was determined from vials containing all components except the hMAO isoforms, which were replaced by a sodium phosphate buffer solution.

Reversibility and Irreversibility Experiments. To evaluate whether some of the tested compounds (**5a**, **5i**, and **5m**) are reversible or irreversible hMAO-B inhibitors, an effective centrifugation-ultrafiltration method (so-called repeated washing) was used.³⁶

Briefly, adequate amounts of the recombinant hMAO-B were incubated together with a single concentration (see Table 2) of the test drugs or the reference inhibitor *R*-(-)-deprenyl in a sodium phosphate buffer (0.05 M, pH 7.4) for 15 min at 37 °C.

After this incubation period, an aliquot of this incubated was stored at 4 °C and used for subsequent measurement of hMAO-B activity under the experimental conditions indicated above (see the section Determination of MAO Activity). The remaining incubated sample (300 μL) was placed in a Ultrafree-0.5 centrifugal tube (Millipore, Billerica, MA) with a 30 kDa Biomax membrane in the middle of the tube and centrifuged (9000g, 20 min, 4 °C) in a centrifuge (J2-MI, Beckman Instruments, Inc., Palo Alto, CA). The enzyme retained in the 30 kDa membrane was resuspended in sodium phosphate buffer at 4 °C and centrifuged again (under the same experimental conditions described above) two successive times. After the third centrifugation, the enzyme retained in the membrane was resuspended in sodium phosphate buffer (300 μL) and an aliquot of this suspension was used for subsequent hMAO-B activity determination.

Control experiments were performed simultaneously (to define 100% hMAO-B activity) by replacing the test drugs with appropriate dilutions of the vehicles. The corresponding values of percent (%) hMAO-B inhibition were separately calculated for samples with and without repeated washing.

Molecular Modeling. The Protein Data Bank³³ (PDB) crystallographic structures 2Z5X³⁴ and 2BK3³⁵ were considered as receptor model of hMAO-A and hMAO-B, respectively.

Compound **5a**, **5i**, and **5m** were built by means of the Maestro GUI³⁷ and, after preliminary optimization, were submitted to 1000 steps of the Monte Carlo search as implemented in MacroModel version 7.2.³⁸ The AMBER* force field³⁹ was adopted for evaluating the energy of all generated conformers, and the GB/SA implicit solvation model⁴⁰ was used to take into account the effects of the aqueous environment. The global minimum energy structure of each compound was considered for the next docking simulations. The crystallographic model of both enzymes required graphical manipulation. The cocrystallized ligands, harmine and farnesol, respectively, for 2Z5X and 2BK3, were removed, FAD double bonds were fixed and hydrogen atoms were added onto both proteins and cofactors.

According to the Glide⁴¹ methodology, a regular box of about 110000 Å³, centered onto the cofactor N5 atom, was considered as the enzyme active site for both hMAO-A and -B models. To take into account the induced fit phenomena, ligands were docked using the “flexible” algorithm.

Because the default Glide scoring function was not in agreement with the pIC₅₀, we adopted the interaction energy (*C*_{vdw}) for evaluating the binding mode of **5a**, **5i**, and **5m**, where we observed a good correlation (*r*² = 0.97) with the experimental pIC₅₀ data (Table 4).

Acknowledgment. This work was supported from MURST (Italy), Ministerio de Sanidad y Consumo (Spain; FISS PI061537),

and Consellería de Innovación e Industria de la Xunta de Galicia (Spain; INCITE07PXI203039ES, INCITE08E1R203054ES, and 08CSA019203PR). Francisco Orallo is especially grateful to the Consellería de Educación y Ordenación Universitaria de la Xunta de Galicia (Spain) for financial support aimed to intensifying his research activity and reducing his teaching during the 2007–2008 academic year [Programa de promoción de intensificación de la actividad investigadora en el sistema Universitario de Galicia (SUG)]. We also acknowledge Anton Gerada, a professional translator, Fellow of the Institute of Translation and Interpreting of London and Member of AIIC (Association Internationale des Interprètes de Conférences, Geneva), for revision of the manuscript.

Supporting Information Available: Analytical and spectral data for new compounds **2–4** and **5a–p** and a few details on pharmacological studies. This material is available free of charge via the Internet at <http://pubs.acs.org>.

References

- (1) Kalgutkar, A. S.; Castagnoli, N., Jr. Selective inhibitors of monoamine oxidase (MAO-A and MAO-B) as probes of its catalytic site and mechanism. *Med. Res. Rev.* **1995**, *15* (4), 325–388.
- (2) Binda, C.; Newton-Vinson, P.; Hubálek, F.; Edmonson, D. E.; Mattevi, A. Structure of human monoamine oxidase B, a drug target for the treatment of neurological disorders. *Nat. Struct. Biol.* **2002**, *9*, 22–26. Data deposition: www.pdb.org (PDB ID code 1GOS).
- (3) De Colibus, L.; Li, M.; Binda, C.; Lustig, A.; Edmonson, D. E.; Mattevi, A. Three-dimensional structure of human monoamine oxidase A (MAO A): Relation to the structures of rat MAO A and human MAO B. *Proc. Natl. Acad. Sci. U.S.A.* **2005**, *102*, 12684–12689. Data deposition: www.pdb.org (PDB ID code 2BXR, 2BXS, and 2BYB).
- (4) Strolin-Benedetti, M.; Dostert, P. Monoamine oxidase: from physiology and pathophysiology to the design and clinical application of reversible inhibitors. *Adv. Drug Res.* **1992**, *23*, 65–125.
- (5) (a) Carreiras, M. C.; Marco, J. L. Recent approaches to novel anti-Alzheimer therapy. *Curr. Pharm. Des.* **2004**, *10* (25), 3167–3175. (b) Fernández, H. H.; Chen, J. J. Monoamine oxidase-B inhibition in the treatment of Parkinson's disease. *Pharmacotherapy* **2007**, *27*, 174S–185S. (c) Factor, S. A. Current status of symptomatic medical therapy in Parkinson's disease. *Neurotherapeutics* **2008**, *5* (2), 164–180. (d) Santana, L.; González-Diáz, H.; Quezada, E.; Uriarte, E.; Yañez, M.; Vinã, D.; Orallo, F. Quantitative Structure–Activity Relationship and Complex Network Approach to Monoamine Oxidase A and B Inhibitors. *J. Med. Chem.* **2008**, *51* (21), 6740–6751.
- (6) Pacher, P.; Kecskemeti, V. Trends in the development of new antidepressants. Is there a light at the end of the tunnel? *Curr. Med. Chem.* **2004**, *11* (7), 925–943.
- (7) Bolasco, A.; Fioravanti, R.; Carradori, S. Recent development of monoamine oxidase inhibitors. *Expert Opin. Ther. Pat.* **2005**, *15* (12), 1763–1782.
- (8) Shih, J. C.; Chen, K.; Ridd, M. J. Monoamine oxidase: from genes to behaviour. *Annu. Rev. Neurosci.* **1999**, *22*, 197–217.
- (9) Mellick, G. D.; Buchanan, D. D.; McCann, S. J.; James, K. M.; Johnson, A. G.; Davis, D. R.; Liyou, N.; Chan, D.; Le Couteur, D. G. Variations in the monoamine oxidase B (MAO B) gene are associated with Parkinson's disease. *Movement Disord.* **1999**, *14*, 219–224.
- (10) (a) Barnham, K. J.; Masters, C. L.; Bush, A. I. Neurodegenerative diseases and oxidative stress. *Nat. Rev. Drug Discovery* **2004**, *3*, 205–214. (b) Sayre, L. M.; Perry, G.; Smith, M. A. Oxidative Stress and Neurotoxicity. *Chem. Res. Toxicol.* **2008**, *21*, 172–188.
- (11) Youdim, M. B. H.; Fridkin, M.; Zheng, H. Novel bifunctional drugs targeting monoamine oxidase inhibition and iron chelation as an approach to neuroprotection in Parkinson's disease and other neurodegenerative diseases. *J. Neural Transm.* **2004**, *111*, 1455–1471.
- (12) Go, M. L.; Wu, X.; Liu, X. L. Chalcones: an update on cytotoxic and chemoprotective properties. *Curr. Med. Chem.* **2005**, *12*, 481–499.
- (13) Dimmock, J. R.; Elias, D. W.; Beazely, M. A.; Kandepu, N. M. Bioactivities of chalcones. *Curr. Med. Chem.* **1999**, *6*, 1125–49.
- (14) Batovska, D.; Parushev, St.; Slavova, A.; Bankova, V.; Tsvetkova, I.; Ninova, M.; Najdenski, H. Study on the substituents' effects of a series of synthetic chalcones against the yeast *Candida albicans*. *Eur. J. Med. Chem.* **2007**, *42*, 87–92.
- (15) Lahtchev, K. L.; Batovska, D. I.; Parushev, St. P.; Ubiyovkov, V. M.; Sibirny, A. A. Antifungal activity of chalcones: A mechanistic study using various yeast strains. *Eur. J. Med. Chem.* **2008**, *43*, 2220–2228.

- (16) Trivedi, J. C.; Bariwal, J. B.; Upadhyay, K. D.; Naliapara, Y. T.; Soshi, S. K.; Pannecouque, C. C.; De Clercq, E.; Shah, A. K. Improved and rapid synthesis of new coumarinyl chalcone derivatives and their antiviral activity. *Tetrahedron Lett.* **2007**, *48*, 8472–8474.
- (17) Tabata, K.; Motani, K.; Takayanagi, N.; Nishimura, R.; Asami, S.; Kimura, Y.; Ukiya, M.; Hasegawa, D.; Akihisa, T.; Suzuki, T. Xanthoangelol, a major chalcone constituent of *Angelica keiskei*, induces apoptosis in neuroblastoma and leukemia cells. *Biol. Pharm. Bull.* **2005**, *28*, 1404–1407.
- (18) Kimura, Y.; Baba, K. Antitumor and antimetastatic activities of *Angelica keiskei* roots, part 1: Isolation of an active substance, xanthoangelol. *Int. J. Cancer* **2003**, *106*, 429–37.
- (19) Cheng, Z. J.; Lin, C. N.; Hwang, T. L.; Teng, C. M. Brousochalcone A, a potent antioxidant and effective suppressor of inducible nitric oxide synthase in lipopolysaccharide-activated macrophages. *Biochem. Pharmacol.* **2001**, *61*, 939–946.
- (20) Rojas, J.; Domínguez, J. N.; Charris, J. E.; Lobo, G.; Payá, M.; Ferrandiz, M. L. Synthesis and inhibitory activity of dimethylamino-chalcone derivatives on the induction of nitric oxide synthase. *Eur. J. Med. Chem.* **2002**, *37*, 699–705.
- (21) Takahashi, T. T.; Takasuka, N.; Ligo, M.; Baba, M.; Nishino, H.; Tsuda, H.; Okuyama, T. Isoliquiritigenin, a flavonoid from licorice, reduces prostaglandin E₂ and nitric oxide, causes apoptosis, and suppresses aberrant crypt foci development. *Cancer Sci.* **2004**, *95*, 448–453.
- (22) Israf, D. A.; Khaizurin, T. A.; Syhida, A.; Lajis, N. H.; Khozirah, S. Cardamonin inhibits COX and iNOS expression via inhibition of p65NF- μ B nuclear translocation and I κ -B phosphorylation in RAW 264.7 macrophage cells. *Mol. Immunol.* **2007**, *44*, 673–679.
- (23) Kim, Y. H.; Kim, J.; Park, H.; Kim, H. P. Anti-inflammatory Activity of the Synthetic Chalcone Derivatives: Inhibition of Inducible Nitric Oxide Synthase-Catalyzed Nitric Oxide Production from Lipopolysaccharide-Treated RAW 264.7 Cells. *Biol. Pharm. Bull.* **2007**, *30* (8), 1450–1455.
- (24) Ngameni, B.; Watchueng, J.; Boyom, F. F.; Keumedjio, F.; Ngadjui, B. T.; Gut, J.; Abegaz, B. M.; Rosenthal, P. J. Antimalarial prenylated chalcones from the twigs of *Dorstenia barteri* var *subtriangularis*. *ARKIVOC* **2007**, *xiii*, 116–123.
- (25) Santos, L.; Curi Pedrosa, R.; Correa, R.; Filho, V. C.; Nunes, R. J.; Yunes, R. A. Biological Evaluation of Chalcones and Analogues as Hypolipidemic Agents. *Arch. Pharm. Chem. Life Sci.* **2006**, *339*, 541–546.
- (26) Orallo, F. *trans*-Resveratrol: a magical elixir of eternal youth. *Curr. Med. Chem.* **2008**, *15*, 1887–1898.
- (27) Howitz, K. T.; Bitterman, K. J.; Cohen, H. Y.; Lamming, D. W.; Lavu, S.; Wood, J. G.; Zipkin, R. E.; Chung, P.; Kisielewski, A.; Zhang, L. L.; Scherer, B.; Sinclair, D. A. Small molecule activators of sirtuins extend *Saccharomyces cerevisiae* lifespan. *Nature* **2003**, *425*, 191–196.
- (28) (a) Haraguchi, H.; Tanaka, Y.; Kabbash, A.; Fujioka, T.; Ishizu, T.; Yagi, A. Monoamine oxidase inhibitors from *Gentiana lutea*. *Phytochemistry* **2004**, *65*, 2255–2260. (b) Jamal, H.; Ansari, W. H.; Rizvi, S. J. Evaluation of chalcones-a flavonoid subclass for their anxiolytic effect in rats using elevated plus maze and open field behaviour tests. *Fund. Clin. Pharmacol.* **2008**, *22*, 673–681. (c) Tanaka, S.; Kuwai, Y.; Tabata, M. Isolation of Monoamine Oxidase Inhibitors from *Glycyrrhiza uralensis* Roots and the Structure–Activity Relationship. *Planta Med.* **1987**, *53*, 5–8.
- (29) Chimenti, F.; Bolasco, A.; Manna, F.; Secci, D.; Chimenti, P.; Granese, A.; Befani, O.; Turini, P.; Cirilli, R.; La Torre, F.; Alcaro, S.; Ortuso, F.; Thierry, L. Synthesis, biological evaluation and 3D-QSAR of 1,3,5-trisubstituted-4,5-dihydro-(1*H*)-pyrazole derivatives as potent and highly selective monoamine oxidase A inhibitors. *Curr. Med. Chem.* **2006**, *13*, 1411–1428.
- (30) Chimenti, F.; Fioravanti, R.; Bolasco, A.; Manna, F.; Chimenti, P.; Secci, D.; Befani, O.; Turini, P.; Ortuso, F.; Alcaro, S. Monoamine Oxidase Isoform-Dependent Tautomeric Influence in the Recognition of 3,5-Diaryl Pyrazole Inhibitors. *J. Med. Chem.* **2007**, *50*, 425–428.
- (31) Chimenti, F.; Fioravanti, R.; Bolasco, A.; Manna, F.; Chimenti, P.; Secci, D.; Rossi, F.; Turini, P.; Ortuso, F.; Alcaro, S.; Cardia, M. C. Synthesis, molecular modeling studies and selective inhibitory activity against MAO of *N*1-propanoyl-3,5-diphenyl-4,5-dihydro-(1*H*)-pyrazole derivatives. *Eur. J. Med. Chem.* **2008**, *43*, 2262–2267.
- (32) Yáñez, M.; Fraiz, N.; Cano, E.; Orallo, F. Inhibitory effects of *cis*- and *trans*-resveratrol on noradrenaline and 5-hydroxytryptamine uptake and on monoamine oxidase activity. *Biochem. Biophys. Res. Comm.* **2006**, *344*, 688–695.
- (33) Berman, H. M.; Westbrook, J.; Feng, Z.; Gilliland, G.; Bhat, T. N.; Weissig, H.; Shindyalov, I. N.; Bourne, P. E. The protein data bank. *Nucleic Acids Res.* **2000**, *28*, 235–242.
- (34) Son, S. Y.; Ma, J.; Kondou, Y.; Yoshimura, M.; Yamashita, E.; Tsukihara, T. Structure of human monoamine oxidase A at 2.2-Å resolution: The control of opening of the entry for substrates/inhibitors. *Proc. Natl. Acad. Sci. U.S.A.* **2008**, *105*, 5739–5744, Data deposition: www.pdb.org (PDB ID code 2Z5X).
- (35) Hubalek, F.; Binda, C.; Khalil, A.; Li, M.; Mattevi, A.; Castagnoli, N.; Edmondson, D. E. Demonstration of Isoleucine 199 as a Structural Determinant for the Selective Inhibition of Human Monoamine Oxidase B by Specific Reversible Inhibitors. *J. Biol. Chem.* **2005**, *280*, 15761–15766, Data deposition: www.pdb.org (PDB ID code 2BK3).
- (36) Chimenti, F.; Maccioni, E.; Secci, D.; Bolasco, A.; Chimenti, P.; Granese, A.; Carradori, S.; Alcaro, S.; Ortuso, F.; Yáñez, M.; Orallo, F.; Cirilli, R.; Ferretti, R.; La Torre, F. Synthesis, Stereochemical Identification, and Selective Inhibitory Activity against Human Monoamine Oxidase-B of 2-Methylcyclohexylidene-(4-arylthiazol-2-yl)hydrazones. *J. Med. Chem.* **2008**, *51*, 4874–4880.
- (37) *Maestro*, version 4.1; Schroedinger Inc.: Portland, OR, 1998–2001.
- (38) Mohamadi, F.; Richards, N. G. J.; Guida, W. C.; Liskamp, R.; Lipton, M.; Caufield, C.; Chang, G.; Hendrickson, T.; Still, W. C. MacroModel—an integrated software system for modeling organic and bioorganic molecules using molecular mechanics. *J. Comput. Chem.* **1990**, *11*, 440–467.
- (39) (a) McDonald, D. Q.; Still, W. C. AMBER torsional parameters for the peptide backbone. *Tetrahedron Lett.* **1992**, *33*, 7743–7746. (b) Weiner, S. J.; Kollman, P. A.; Case, D. A.; Singh, U. C.; Chio, C.; Alagona, G.; Profeta, S.; Weiner, P. A new force field for molecular mechanical simulation of nucleic acids and proteins. *J. Am. Chem. Soc.* **1984**, *106*, 765–784.
- (40) Hasel, W.; Hendrickson, T. F.; Still, W. C. A rapid approximation to the solvent-accessible surface areas of atoms. *Tetrahedron Comput. Methodol.* **1988**, *1*, 103–116.
- (41) (a) *Glide*, version 4.1; Schroedinger Inc.: Portland, OR, 1998–2001; (b) Eldridge, M. D.; Murray, C. W.; Auton, T. R.; Paolini, G. V.; Mee, R. P. Empirical scoring functions: I. The development of a fast empirical scoring function to estimate the binding affinity of ligands in receptor complexes. *J. Comput.-Aided Mol. Des.* **1997**, *11*, 425–445.

JM801590U